

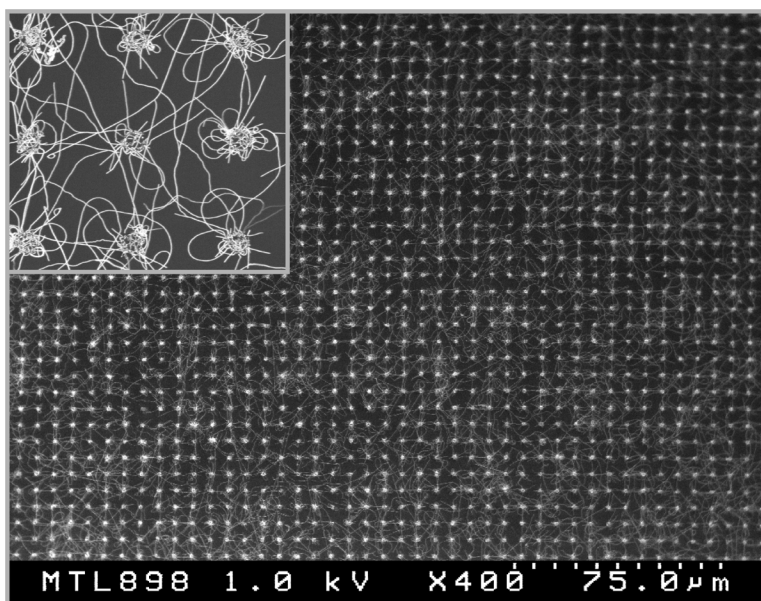
## Communication

### High-Quality Single-Walled Carbon Nanotubes with Small Diameter, Controlled Density, and Ordered Locations Using a Polyferrocenylsilane Block Copolymer Catalyst Precursor

Jennifer Q. Lu, Thomas E. Kopley, Nick Moll, Daniel Roitman, Danielle Chamberlin, Qiang Fu, Jie Liu, Thomas P. Russell, David A. Rider, Ian Manners, and

*Chem. Mater.*, **2005**, 17 (9), 2227-2231 • DOI: 10.1021/cm048030e

Downloaded from <http://pubs.acs.org> on January 1, 2009



## More About This Article

Additional resources and features associated with this article are available within the HTML version:

- Supporting Information
- Links to the 31 articles that cite this article, as of the time of this article download
- Access to high resolution figures
- Links to articles and content related to this article
- Copyright permission to reproduce figures and/or text from this article

[View the Full Text HTML](#)



**ACS Publications**  
High quality. High impact.

# High-Quality Single-Walled Carbon Nanotubes with Small Diameter, Controlled Density, and Ordered Locations Using a Polyferrocenylsilane Block Copolymer Catalyst Precursor

Jennifer Q. Lu,<sup>\*,†</sup> Thomas E. Kopley,<sup>†</sup> Nick Moll,<sup>†</sup> Daniel Roitman,<sup>†</sup> Danielle Chamberlin,<sup>†</sup> Qiang Fu,<sup>‡</sup> Jie Liu,<sup>‡</sup> Thomas P. Russell,<sup>§</sup> David A. Rider,<sup>||</sup> Ian Manners,<sup>||</sup> and Mitchell A. Winnik<sup>||</sup>

Agilent Laboratories, 3500 Deer Creek Road, Palo Alto, California 94304, Chemistry Department, Duke University, Durham, North Carolina 27708, Department of Polymer Science and Engineering, University of Amherst, Amherst, Massachusetts 01003, and Chemistry Department, University of Toronto, Toronto, Ontario, Canada M5S 3H6

Received November 9, 2004

Revised Manuscript Received March 15, 2005

Carbon nanotubes (CNTs), with their exceptional electrical properties, chemical stability, and mechanical strength, have attracted a great deal of attention. This makes the material attractive for a wide range of applications, including composite materials,<sup>1</sup> battery electrode materials,<sup>2</sup> nanoelectronics,<sup>3,4</sup> and nanoscale sensors.<sup>5</sup> However, the properties of CNTs are highly dependent on their structure and size. Such sensitivity to size and structure imposes a potential barrier to the realization of the novel properties of CNTs in many applications. In the growth of CNTs by chemical vapor deposition (CVD), the diameters of CNTs are determined by the sizes of catalysts.<sup>6</sup> One way to obtain CNTs with fewer chiral arrangements is to use smaller catalyst particles. Thus, CNTs with smaller diameters, for example less than 2 nm, are most likely to be single-walled with fewer geometrical arrangements. This should limit the band gap range and allow the possibility of having all metallic or all semiconducting CNTs from a given growth. Moreover, such small-diameter nanotubes have larger band gaps, which minimize off-state leakage, thereby increasing the transistor on/off current ratio in transistor applications.<sup>7</sup> Significant progress has been made in driving catalyst size, and thus nanotube diameters, down

into the subnanometer range. Using plasma-enhanced CVD (PECVD), Li and co-workers have grown nanotubes with diameters ranging from 0.8 to 1.5 nm.<sup>8</sup> More recently, the NEC group has announced  $1.3 \pm 0.4$  nm diameter nanotubes using conventional CVD.<sup>9</sup> However, to the best of our knowledge, no previously published method has demonstrated that uniformly distributed CNTs or lithographic selectively grown CNTs with tube diameters around or less than 1 nm can be produced over a large surface area.

One promising route to synthesize catalysts with controlled size and spacing for CNT growth is to use diblock copolymers where one of the blocks contains the catalyst metal and the other is a non-metal-containing block.<sup>10</sup> Polystyrene-*b*-polyferrocenylsilane (PS-PFEMS) diblock copolymers have been reported as iron catalyst precursors capable of generating single-walled CNTs and multiwalled CNTs.<sup>11,12</sup> In this communication, we utilized the self-assembling ability of PS-PFEMS diblock copolymer to generate controlled size and periodically spaced PFEMS cylinders in a polystyrene matrix.<sup>13</sup> Following UV-ozonation and thermolysis at 700 °C in air, PFEMS mineralizes to form iron nanoparticles in a silicon-based ceramic matrix. The ceramic matrix reduces the agglomeration of the iron nanoparticles, allowing the growth of CNTs with diameters of 1 nm or less. Combining this characteristic with the excellent processability of the polymer material, we have been able to produce uniformly distributed carbon nanotube networks. More importantly, we have successfully demonstrated that this catalytic system can be used to generate patterned catalytic islands for selective growth of carbon nanotubes at predefined locations over a large surface area.

For the experiments described herein, iron-containing nanostructures for carbon nanotube growth were prepared from spin-coated films of PS-PFEMS (chemical formula as shown in the inserted Figure 1), which was synthesized via sequential living anionic polymerization.<sup>14</sup> A combination of gel permeation chromatography and <sup>1</sup>H NMR revealed that the mean number of repeat units of PS was 263 and that of PFEMS was 44, giving an approximate volume fraction of PFEMS of 25%. The polymer molecular weight

\* To whom correspondence should be addressed. E-mail: Jennifer\_lu@agilent.com. Tel.: 650-485-3714. Fax: 650-485-8626.

<sup>†</sup> Agilent Laboratories.

<sup>‡</sup> Duke University.

<sup>§</sup> University of Amherst.

<sup>||</sup> University of Toronto.

- (1) Huxtable, S. T.; Cahill, D. G.; Shenogin, S.; Xue, L. P.; Ozisik, R.; Barone, P.; Usrey, M.; Strano, M. S.; Siddons, G.; Shim, M.; Keblinski, P. *Nature Mater.* **2003**, *2*, 731.
- (2) Honda, K.; Yoshimura, M.; Kawakita, K.; Fujishima, A.; Sakamoto, Y.; Yasui, K.; Nishio, N.; Masuda, H. *J. Electrochem. Soc.* **2004**, *151*, A532.
- (3) Appenzeller, J.; Knoch, J.; Martel, R.; Derycke, V.; Wind, S. J.; Avouris, P. *IEEE Trans. Nanotechnol.* **2002**, *1*, 184.
- (4) McEuen, P. L.; Fuhrer, M. S.; Park, H. K. *IEEE Trans. Nanotechnol.* **2002**, *1*, 78.
- (5) Chen, R. J.; Bangsaruntip, S.; Drouvalakis, K. A.; Kam, N. W. S.; Shim, M.; Li, Y. M.; Kim, W.; Utz, P. J.; Dai, H. J. *Proc. Natl. Acad. Sci. U.S.A.* **2003**, *100*, 4984.
- (6) Li, T.; Kim, W.; Zhang, Y.; Rolandi, M.; Wang, D.; Dai, H. J. *Phys. Chem. B* **2001**, *105*, 11424.
- (7) Guo, J.; Javey, A.; Dai, H.; Datta, S.; Lundstrom M.; cond-mat/0309039, 2003.

- (8) Li, Y. M.; Mann, D.; Rolandi, M.; Kim, W.; Ural, A.; Hung, S.; Javey, A.; Cao, J.; Wang, D. W.; Yenilmez, E.; Wang, Q.; Gibbons, J. F.; Nishi, Y.; Dai, H. J. *Nano Lett.* **2004**, *4*, 317.
- (9) Electronic Engineering Time, Sep 7th, 2004
- (10) Lu, J.; Bai, J.; Moll, N.; Roitman, D.; Yang, D.; Fu, Q.; Liu, J.; Rider, D.; Manners, I.; Winnik, M. Submitted to the 2004 Fall MRS proceedings.
- (11) (a) Lastella, S.; Jung, Y. J.; Yang, H. C.; Vajtai, R.; Ajayan, P. M.; Ryu, C. Y.; Rider, D. A.; Manners, I. *J. Mater. Chem.* **2004**, *14*, 1791. (b) Hinderling, C.; Keles, Y.; Stockli, T.; Kanpp, H. E.; de los Arocs, T.; Olehafen, P.; Korczagin, T.; Hempenius, M. A.; Vancso, G. J.; Pugin, R. L.; Heinzelmann, H. *Adv. Mater.* **2004**, *16*, 876.
- (12) For related work using polyvinylferrocene random copolymers see Lahiff, E.; Ryu, C. Y.; Currant S.; Minett A. I.; Blau W. J.; Ajayan P. M. *Nano Lett.* **2004**, *3*, 1333.
- (13) Temple, K.; Kulbaba, K.; Power-Billard, K. N.; Manners, I.; Leach, K. A.; Xu, T.; Russell, T. P.; Hawker, C. J. *Adv. Mater.* **2003**, *15*, 297.
- (14) (a) Temple, K.; Massey, J. A.; Chen, Z.; Vaidya, N.; Berenbaum, A.; Foster, M. D.; Manners, I. *J. Inorg. Organomet. Polym.* **1999**, 189. (b) Rider, D. A.; Power-Billard, K. N.; Cavicchi, K. A.; Russell, T. P.; Manners, I. Submitted to *Macromolecules*.

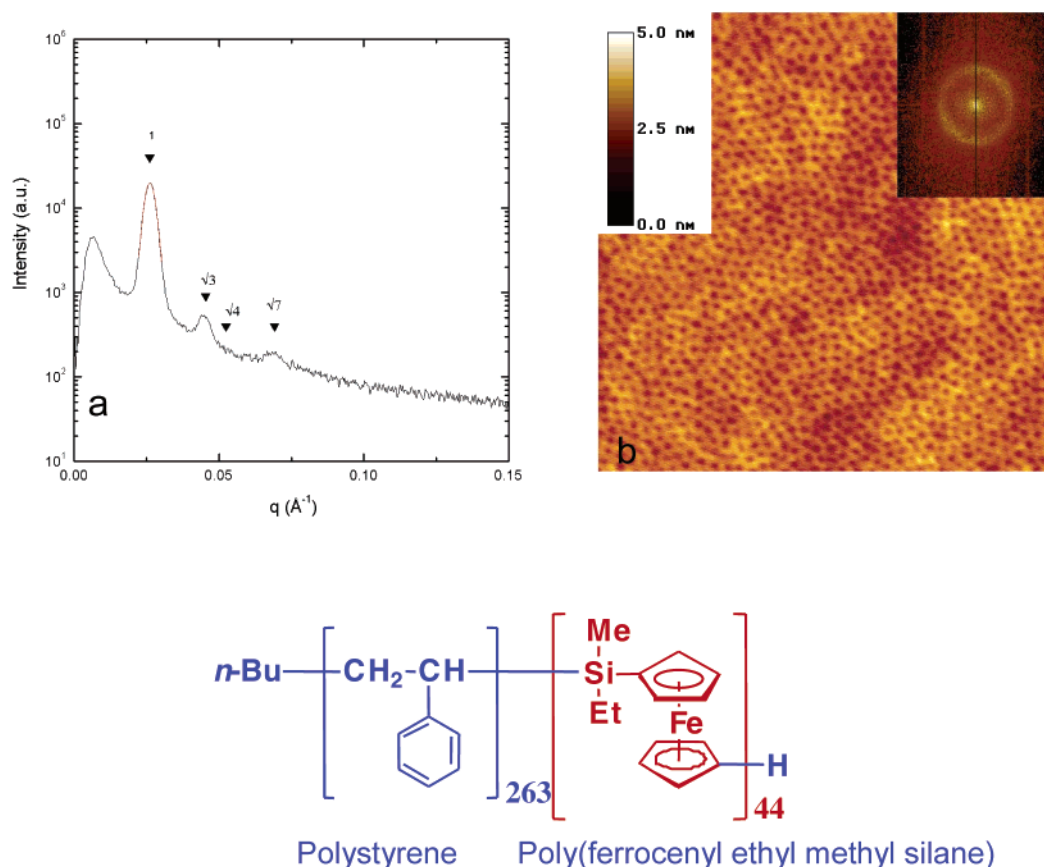


**Figure 1.** (a) Small-angle X-ray scattering profile of bulk PS-*b*-PFEMS. (b) AFM height image of spin-coated PS-*b*-PFEMS film after annealing.

( $M_n$ ) was 38700 with a polydispersity of 1.01. Bulk morphological studies using small-angle X-ray scattering on the material confirmed that the block copolymer forms PFEMS cylinders in a PS matrix during annealing as seen in Figure 1a.

For full-film carbon nanotube growth, a PS-PFEMS film with a film thickness of 15 nm was prepared by spin casting at 4000 rpm for 30 s from a dilute toluene solution onto a 500 nm thermal oxide layer on silicon and quartz substrates. After coating, the samples were annealed. The surface morphology of the spin-coated thin polymer film after annealing was characterized by atomic force microscopy (AFM). The AFM image in Figure 1b indicates that the film exhibits a periodically ordered hexagonal morphology with cylindrical PFEMS domains embedded in a PS matrix oriented perpendicular to the substrate. The domain size of PFEMS is about 15.8 nm with a spacing of 30.1 nm based on 2D Fourier transform analysis. Due to the well-ordered structure generated in the diblock polymer film by spin-coating, precise control of size and periodicity of the iron-containing nanostructures was thus obtained. The process is simple, needing no additional tool settings, and is fully compatible with standard device-fabrication processes. After annealing, UV-ozone treatment was carried out to remove organic components and convert nonvolatile inorganic components into  $\text{SiO}_2$  and  $\text{Fe}_2\text{O}_3$  as confirmed by X-ray photoelectron spectral analysis.

After thermolysis at 700 °C in air, the carbon nanotube growth was carried out in a CVD system as described previously<sup>15</sup> and the thin film-coated substrate was heated

to 900 °C under 500 sccm  $\text{H}_2$ . Subsequently, a mixture of 800 sccm  $\text{CH}_4$  and 20 sccm  $\text{C}_2\text{H}_4$  was added to the gas flow to initiate carbon nanotube growth. The growth time was 10 min. After the growth, the feed of  $\text{CH}_4$  and  $\text{C}_2\text{H}_4$  was switched off and the furnace was cooled to room temperature under a flow of  $\text{H}_2$ . Figure 2 shows a representative scanning electron microscope (SEM) image of the substrate after the CVD growth. It depicts a semi-ordered CNT network [subsequently referred to as CNT mat] at both high (inset) and low magnification. Raman analysis was performed to examine the overall quality of the CNTs on a thermal oxide substrate. The excitation source was a 20 mW, 488 nm laser with a spot size of 25  $\mu\text{m}$ . The integration time was approximately 20 s for each spectrum. A typical Raman spectra of CNTs is displayed in Figure 3. The D band at 1380  $\text{cm}^{-1}$  is the second-order defect-induced Raman mode involving one phonon elastic scattering process. Thus, the intensity of this peak is directly correlated with the level of defects or dangling bonds in the  $\text{sp}^2$  arrangement of graphene. The G band centered at 1590  $\text{cm}^{-1}$  is the first-order Raman process attributed to an in-plane oscillation of carbon atoms in the  $\text{sp}^2$  graphene sheet.<sup>16–18</sup> The very low intensity of the D band signal, and narrow width and high intensity of the

- (15) Fu, Q.; Huang, S. M.; Liu, J. J. *Phys. Chem. B* **2004**, *108*, 6124.
- (16) Dresselhaus, M. S.; Eklund, P. C. *Adv. Phys.* **2000**, *49*, 705.
- (17) Dresselhaus G.; Dresselhaus, M. S. In *Science and Applications of Nanotubes*; Tománek, D., Enbody, R. J., Eds.; Kluwer Academic: New York, 2000; p 275.
- (18) Rao, A. M.; Chen, J.; Richter, E.; Schlecht, U.; Eklund, P. C.; Haddon, R. C.; Venkateswaran, U. D.; Kwon, Y. K.; Tomanek, D. *Phys. Rev. Lett.* **2001**, *86*, 3895.



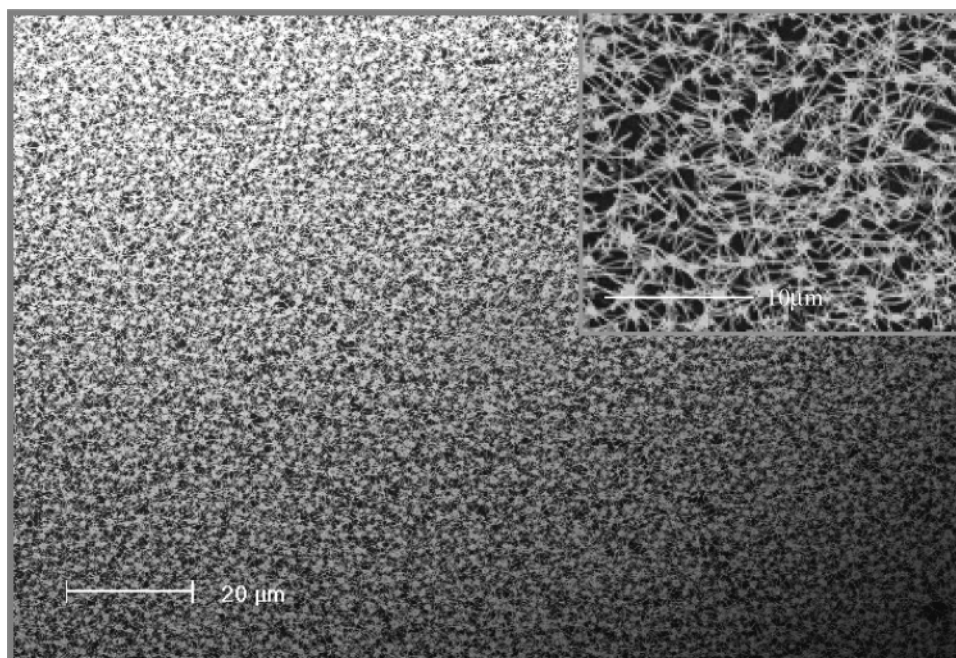


Figure 2. Low- and high-magnification SEM images showing a highly uniform CNT mat.

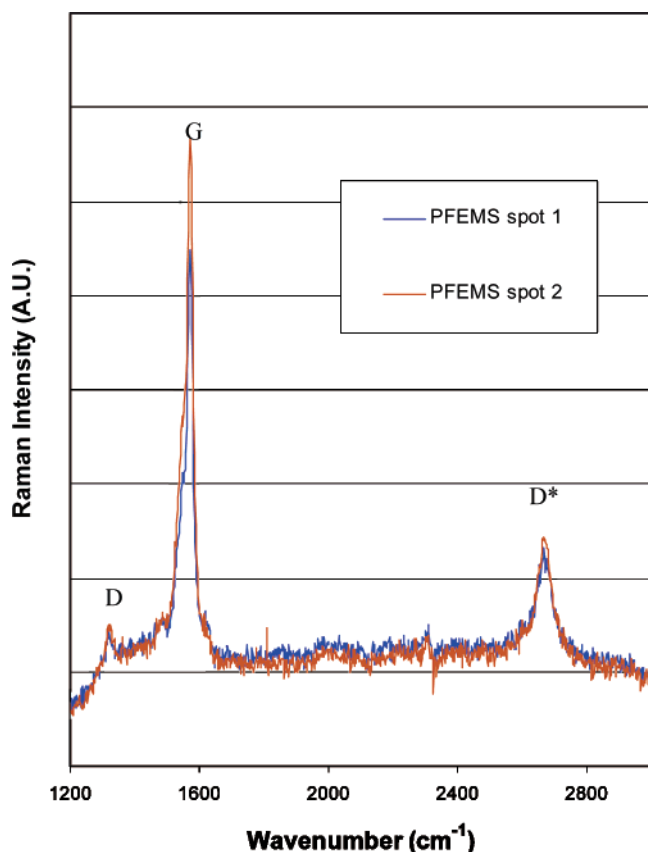


Figure 3. Raman spectra of a single-walled CNT mat at high frequency. G band signal, indicate that the CNTs have very low defect and dangling bond density. This is also supported by the strong intensity of the D\* band at  $2760\text{ cm}^{-1}$ , which is the result of an inelastic two phonon double resonance emission process.

Micro-Raman spectroscopy around the radial-breathing mode (RBM) frequency,  $\omega_{\text{RBS}}$ , was used to obtain the diameters of the carbon nanotubes. In this experiment, CNTs grown on a quartz substrate were used for the analysis.

Raman scattering at lower energy corresponds to the radial-breathing vibrational modes with A1 g symmetry.<sup>16–18</sup> This unique characteristic can only be observed in nanotubes with one or a few walls. The analysis characterized the carbon nanotubes over a  $\sim 1\text{ }\mu\text{m}^2$  area using a 2.0 mW, 632 nm laser. The integration time was 20 min for each spectrum. The tube diameters are estimated using the relationship  $d(\text{nm}) = 233/\omega_{\text{RBS}}$ . The overlapping of tubes produces a slight shift in the Raman RBM frequency.<sup>18</sup> This effect is ignored in the calculation of tube diameters. AFM height measurement of tubes lying on the substrate was also used to estimate the diameters. The majority of the CNTs have diameters around 0.7 nm as shown in Figure 4.

It is well-established that the diameters of CNTs depend on the diameters of the catalysts. Typically, single-walled CNTs are grown at a temperature higher than  $800\text{ }^\circ\text{C}$ . It is evident that catalysts such as iron nanoparticles agglomerate at such high temperatures.<sup>19,20</sup> Many attempts have been made to reduce the agglomeration of iron catalytic nanoparticles at highly elevated temperatures by using either porous materials such as porous  $\text{SiO}_2$ ,  $\text{Al}_2\text{O}_3$ , and zeolite or  $\text{Al}_2\text{O}_3$  and MgO powders. However, the aforementioned methods are not compatible with the integration of CNT synthesis with device fabrication. Furthermore, these methods result in a broad distribution of CNT diameters since there are no self-limiting mechanisms to control the diameters of the nanocatalysts. In our approach, self-assembly precisely controls the size and spacing of PFEMS blocks. UV–ozonation transforms the ferrocenyl unit in the PFEMS segment into iron oxide while the alkyl silane unit turns into  $\text{SiO}_2$ . We hypothesize that iron-rich clusters surrounded by  $\text{SiO}_2$  limit the mobility and coalescence of clusters at the

(19) Klinker, C.; Bonard, J.; Kern, K. ArXiv: cond-mat/0307197, July 9th, 2003.

(20) Ginzburg, M.; MacLachlan, M. J.; Yang, S. M.; Coombs, N.; Coyle, T. W.; Raju, N. P.; Greedan, J. E.; Herber, R. H.; Ozin, G. A.; Manners, I. *J. Am. Chem. Soc.* **2002**, *124*, 2625.

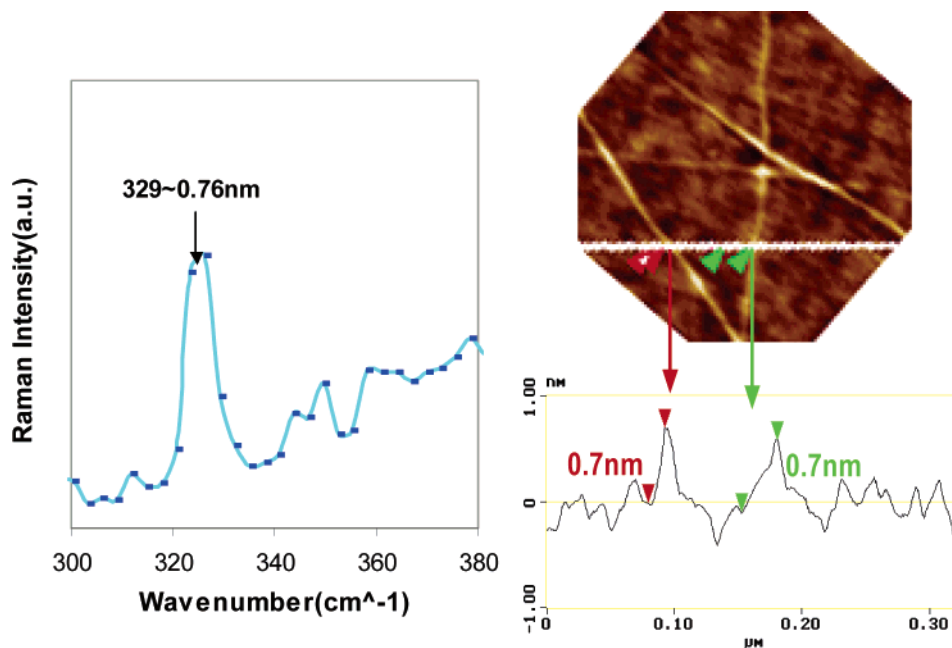


**Figure 4.** Raman spectra of a CNT mat at radial-breathing region and AFM image and height profile of carbon nanotubes.

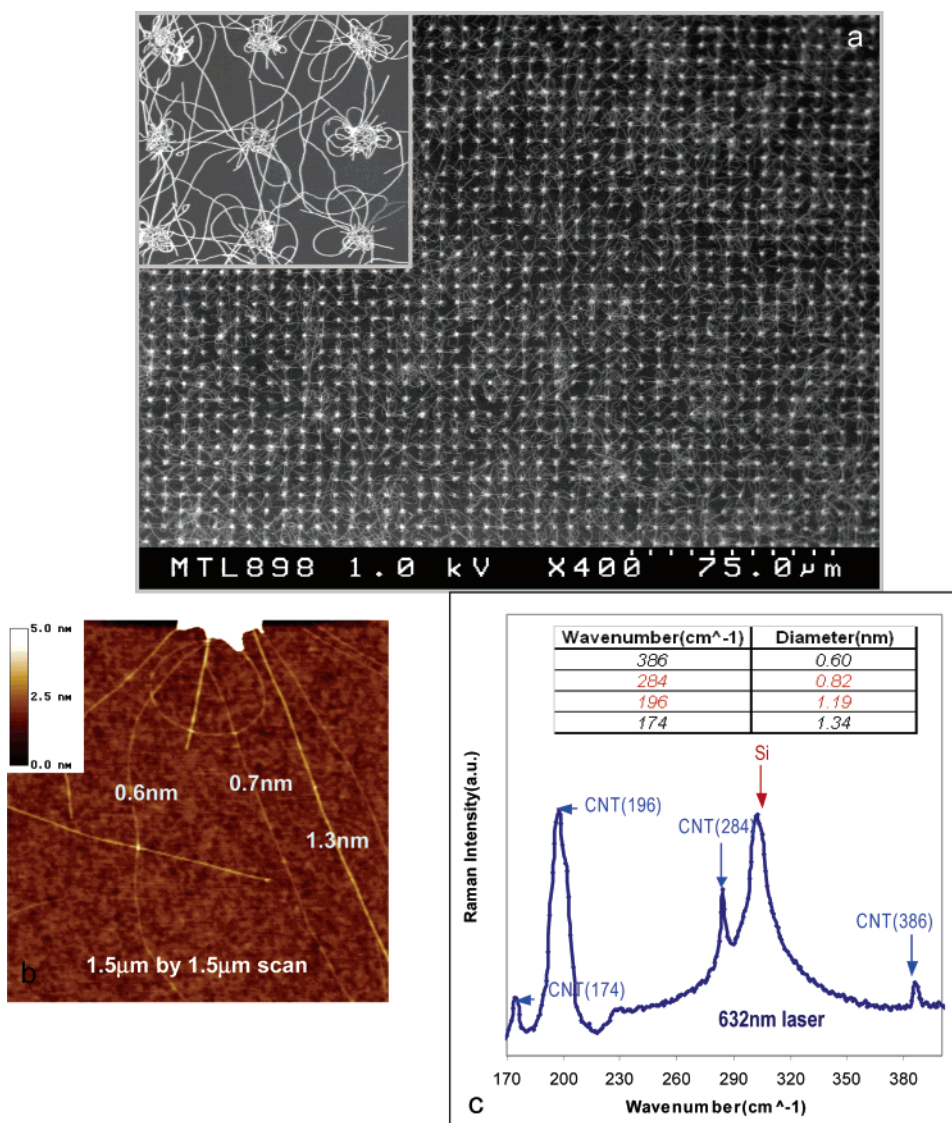


**Figure 5.** (a) SEM images of single-walled CNTs grown from patterned catalytic islands. (b) AFM height image of CNTs from a patterned catalytic island. (c) Raman spectra at the radial-breathing region.

growth temperature, resulting in CNTs with smaller diameter and narrower size distribution than previously reported using conventional CVD methods.

For patterned carbon nanotube growth, a bilayer lift-off process was used to generate patterned catalyst surfaces. Shipley LOL1000 was spun onto a thermal-oxide-coated silicon wafer and then baked at 180 °C for 10 min to give a film with thickness of 60 nm. Subsequently, an 800 nm thick OCG 825 resist film was formed on top of the LOL1000 layer by spin-coating and baked at 105 °C for 3 min. This bilayer system was exposed using an ASML2500/40 stepper with an exposure wavelength of 365 nm and subsequently developed in a metal ion free aqueous base developer. After the patterns were created on a substrate, a PS–PFEMS diblock polymer solution was deposited by spin-coating. After proper annealing, the resist and underlayer structures were then removed by a solvent lift-off. A similar UV–ozone process was used to produce iron-containing silicon oxide nanostructures. Due to the excellent thin film formation capability of this polymer system and the ability of the polymer to re-flow into topographic features such as holes, patterned islands of PS–PFEMS with uniform height were generated.

Optical inspection on three-inch wafers showed that the solvent lift-off process completely removed all materials, leaving only the catalytic islands behind. CNTs were grown using similar CVD conditions to that described above except that the growth time was reduced from 10 to 5 min. The SEM images in Figure 5a depict arrays of carbon nanotubes grown from lithographically defined 0.9  $\mu\text{m}$  catalytic islands over a large surface area. There is no evidence of nanotube growth initiated in the regions between the catalytic islands, indicating that the lift-off process is a very effective means to generate patterned catalyst substrates. The process is very simple and compatible with common semiconductor lithographic processes. The AFM height image in Figure 5b and Raman analysis at the radial breathing mode as shown in Figure 5c indicate that the majority of tubes have diameters

of 1 nm or less. However, a few tubes with large diameters are also found. On average, around 15 CNTs are emitted from a 0.9  $\mu\text{m}$  catalytic island. Smaller islands produce fewer CNTs and so the number of CNTs can be adjusted by the size of the catalyst island.

In summary, we have demonstrated that iron clusters prepared from the PS–PFEMS diblock polymer are very effective catalysts for single-walled carbon nanotube growth. Unlike other catalytic systems which have a very limited shelf life and must be prepared and used immediately, the diblock copolymer forms a relatively stable solution. Thin films prepared from this polymer system are capable of self-assembling into PFEMS columns embedded in a PS matrix. The presence of silicon in the iron-containing polymer segment appears to reduce the aggregation of iron nanoparticles at the growth temperature. Uniformly distributed single-walled carbon nanotubes with diameters of 1 nm or less have been produced by this approach. Patterned catalyst islands can be readily generated using conventional semiconductor processing. Sub-nanometer single-walled carbon nanotubes have been successfully grown on the lithographically predefined catalyst patterns over a very large area. The process can be readily integrated into semiconductor device fabrication and extended to any wafer format for spatially selective growth of SWNTs.

**Acknowledgment.** Nick Moll would like to thank Rolf Jaeger for management support. Jennifer Lu would like to thank Rolf Jaeger for help in preparing the manuscript and Grant Girolami's SEM work. Ian Manners would like to thank the Canadian Government for a Research Chair and to express gratitude to Chang Ryu at Rensselaer Polytechnic Institute for lots of helpful inputs. The work at Duke is in part supported by a NSF-NIRT(NSF-EEC-02-10590) program and the 2002 Young Professor Award from DuPont. The Raman spectroscopy of radial breathing modes was performed at Evans Analytical Group.

CM048030E